Structural Behaviour of Over-Stressed Reinforced Concrete Beams

Charles K. Kankam, William Amankwa-Boahin, Bismark K. Meisuh

Abstract— This present study assessed the structural potential of collapsed beams retrofitted by re-stressing with ordinary low strength steel bars that were end-threaded and tensioned against steel plates at the beam ends by means of tightening nuts. The applied prestress forces were estimated from the central upward deflection of the beams taking into account the downward deflection due selfweight and the short-term prestress losses. Eight stressed beams were subjected to monotonic loading and four to 20 cycles of loading. Four unstressed beams served as control. The ratio of the experimental failure load over the theoretical failure load averaged more than 570% and 380% before and after retrofit respectively. The ratio of the experimental failure load before retrofit, and after retrofit under monotonic loading averaged 70%. There was a 22% increase in the load carrying capacity of the retrofitted beams relative to the unstressed beams. For the stressed beams, the ratio of first crack load over theoretical cracking load averaged 260%. Cyclic loading for the retrofitted beams was characterized by crack closure on removal of the applied load and maximum crack widths were observed to range from 0.08 to 0.70mm while that for the control beams ranged from 2.00 to 4.00mm.

Index Terms— Concrete, Re-stressed beams, Pre-stressed beams, Retrofitted beams.

I. INTRODUCTION

Structural repair and retrofitting is a predominantly cheaper solution to dealing with aging, damaged or failing structures compared to a complete replacement. Steel, concrete, fiber reinforced polymers and many other hosts of engineered materials have been used as wraps, jackets or casings to enhance the structural performance of distressed or damaged structural elements by inducing initial compressive stresses in them [1]–[8]. A study conducted by Kankam [9] to assess the structural behaviour of concrete beams prestressed with ordinary mild steel bars that were post-tensioned by end bolting to induce compressive stresses in the concrete beams, reported significant improvement in the structural behaviour of the stressed beams compared with the unstressed beams. Cracking and failure loads for the stressed beams averaged 280% and 244% of the control unstressed beams. Cyclic loading of the prestressed beams recorded complete crack closure on removal of the applied load.
The aim of the present study was to assess the structural potential of retrofitting over-stressed beams by means of

Charles K. Kankam, Department of Civil Engineering, Kwame Nkrumah University of Science and Technology (KNUST), College of Engineering, Kumasi, Ghana, 00233208168662.
William Amankwa-Boahin, Department of Civil Engineering, Kwame Nkrumah University of Science and Technology (KNUST), College of Engineering, Kumasi, Ghana, 00233244973010.
Bismark K. Meisuh, Department of Civil Engineering, Kwame Nkrumah University of Science and Technology (KNUST), College of Engineering, Kumasi, Ghana, 00233209044586.

tightened anchored steel nuts over threaded reinforcing bars at the beam ends. The load carrying capacity, crack formation and deflection behaviour of the beams were investigated.

II. EXPERIMENTAL PROGRAM

A. Materials and specimens

The concrete comprised ordinary Portland cement, natural river sand and crushed granite stones of maximum size not exceeding 20mm in mix proportions by weight to give two different strengths. The beams measured 125×200mm with an overall span of 1800mm. Reinforcement consisted of diameters 17mm as main bars, 11mm as hanger bars and 5mm as shear reinforcement. Tightening nuts and 8mm thick rigid steel plates measuring 125×200mm were used in the tensioning process. The concrete was mixed in a batch mixer, placed and compacted by means of a vibrator. Curing was done at a 100% relative humidity and approximately 25°C room temperature.

B. Description of beams

Sixteen concrete beams were produced in all. Twelve of the beams (P1 – P12) were post-tensioned using the end-threaded 17mm mild steel bar by tightening nuts against rigid steel plates at the beam ends and four of the beams (C1 – C4) were unstressed to serve as control. The threading at the ends of the bar extended 50mm into the beam to accommodate the elongation of the bar. The bar was inserted through a drilled hole at the ends of the mould, 50mm eccentric to the neutral axis. Reinforcement for the beams was in two series: F-series and S-series. The F-series beams were expected to fail in flexure and had shear reinforcement of diameter 5mm at a spacing of 120mm centers. In addition to the main bar, the F-series beams also had 2no 11mm top and bottom hanger bars. The cross-sectional area of the hanger bars were considered in the calculation of the percentage area of steel reinforcement provided. The S-series beams were expected to fail in shear. They had neither stirrups nor hanger bars (see Fig. 1). A detailed description of the beams is given in Table 1.
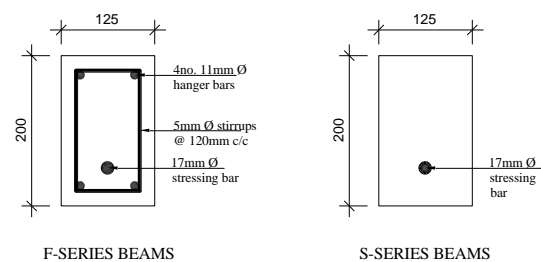

Fig. 1. F-series and S-series beams

Table 1. Description of beams

Beam No.	Span/eff. depth ratio	Concrete strength, f_{cu} (N/mm²)	Modulus of rupture, f_{tc} (N/mm²)	Area of prestressing steel bar, A_p (mm²)	Area of bottom unstressed steel bar, A_u (mm²)	Total area of bottom steel bar, $A_t = A_p + A_u$ (mm²)	$\frac{100*A_t}{bD}$ (%)	Area of top steel bar, A_s' (mm²)	$\frac{100*A_s'}{bD}$ (%)
P1A,F	9.4	22.4	3.2	227	194	421	1.68	194	0.77
P2A,F	9.4	22.4	3.2	227	194	421	1.68	194	0.77
P3B,F	9.4	27.9	4.4	227	194	421	1.68	194	0.77
P4B,F	9.4	27.9	4.4	227	194	421	1.68	194	0.77
P5A,S	10.0	22.4	3.2	227	0	227	0.91	0	0.00
P6A,S	10.0	22.4	3.2	227	0	227	0.91	0	0.00
P7B,S	10.0	27.9	4.4	227	0	227	0.91	0	0.00
P8B,S	10.0	27.9	4.4	227	0	227	0.91	0	0.00
P9A,F	9.4	22.4	3.2	227	194	421	1.68	194	0.77
P10B,F	9.4	27.9	4.4	227	194	421	1.68	194	0.77
P11A,S	10.0	22.4	3.2	227	0	227	0.91	0	0.00
P12B,S	10.0	27.9	4.4	227	0	227	0.91	0	0.00
C1A,F	9.4	22.4	3.2	227	194	421	1.68	194	0.77
C2B,F	9.4	27.9	4.4	227	194	421	1.68	194	0.77
C3A,S	10.0	22.4	3.2	227	0	227	0.91	0	0.00
C4B,S	10.0	27.9	4.4	227	0	227	0.91	0	0.00

C. Stressing of beams

After the beams had attained their 28-day strength, they were arranged on flat beds and the bars tensioned by tightening nut. The prestress forces before and after retrofit were estimated from the resultant upward central deflection of the beam using the equations derived by Kankam [9] and reproduced in Appendix A. The effect of selfweight and prestress losses due to creep and elastic contraction of the concrete, were considered.

D. Test procedure

The beams were simply supported on a rigid steel frame and loaded at its third points to produce a constant moment in the middle one-third region of the spans as seen in Fig. 2. Beams P1 to P8 and C1 to C4 were subjected to monotonic loading, and P9 to P12 to 20 cycles of loading. The stressed beams after failure were re-stressed and reloaded to failure. Crack behaviour and load-deflection data for all load increments were recorded

Fig. 2. Experimental Set-up

III. ESTIMATION OF THEORETICAL LOADS

E. Theoretical first crack load

The first crack load was estimated from the elastic flexural theory based on the modulus of rupture of the unreinforced beam section:

$$M_{cr} = f_{tc}\, bh^2 / 6 \qquad (III.1)$$

where

M_{cr} cracking moment
f_{tc} modulus of rupture
h total depth of the section
b breadth of the section

For a simply supported beam that is subjected to a two point load system and not considering self-weight, the failure load P_{cr} is given by:

$$P_{cr} = 6\, M_{cr} / L \qquad (III.2)$$

where

P_{cr} cracking load
L span

F. Theoretical steel yielding failure load

In accordance with British Standard design code on the structural use of concrete, BS 8110-1 [10], the ultimate limit state at which the unstressed steel yields is given by;

$$M_{ult} = A_s\, f_y\, z \qquad (III.3)$$
$$P_{ult} = 6\, A_s f_y\, z / L \qquad (III.4)$$

where

M_{ult} ultimate moment
P_{ult} failure load
f_y yield stress of steel
A_s steel cross sectional area
z limiting lever arm = $0.775d$
L span
d effective depth of the concrete section

G. Theoretical concrete crushing failure load

In accordance with British Standard BS 8110-1 [10], the ultimate limit state at which the concrete crushes is given by;

$$M_{ult} = 0.156\, f_{cu}\, b\, d^2 \qquad (III.5)$$
$$P_{ult} = 6\, (0.156\, f_{cu}\, b\, d^2) / L \qquad (III.6)$$

where

M_{ult} ultimate moment
P_{ult} failure load
f_{cu} 28-day concrete compressive strength
b breadth of section
d effective depth of concrete section
L span

H. Theoretical Shear Failure Load

Considering the longitudinal unstressed steel bars, the shear reinforcement and the concrete section, The shear failure load in accordance with British Standard BS 8110-1 [10] is given by:

$$A_{sv} = (\,v - v_c\,)\, b_v\, s_v / f_{yv} \qquad (III.7)$$
$$V = [(A_{sv} / s_v)\, f_{yv} + b_v\, v_c\,]\, d \qquad (III.8)$$

where

A_{sv} Area of shear reinforcement
v shear stress
v_c design concrete shear stress
b_v breadth of section
s_v shear reinforcement spacing
f_{yv} area of shear reinforcement
V ultimate shear force

IV. RESULTS AND DISCUSSION

I. Materials and specimens

The average compressive strengths of the concrete were 22 and 28N/mm², with a corresponding modulus of rupture of 3.2 and 4.4N/mm² respectively. The average yield strength test results for reinforcement steel rod was 280 N/mm². Table 2 gives a summary of the theoretical and experimental failure loads. For the stressed beams, the ratio of the first crack load over the theoretical cracking load (P_{cr}/P_{cr}') averaged 260%.

The ratio of the experimental failure loads over the governing theoretical failure loads (P_{ult}/P_{ult}') averaged more than 570% before retrofit and about 380% after retrofit (P_{ult-r}/P_{ult}'). The failure loads of the retrofitted beams averaged 70% of the failure loads before retrofit. The experimental failure load before retrofit and after retrofit saw an average 72% and 25% load increments respectively over the unstressed beams under monotonic loading. The results of the estimation of the applied pre-stress forces before and after collapse are summarized in Tables 3 and 4 respectively.

Table 2. Theoretical and experimental failure loads

Beam No.	Theoretical cracking load, P_{cr}' (kN)	First crack load, P_{cr} (kN)	Exp. failure load, P_{ult} (kN)	Exp. failure load of retrofitted beam, P_{ult-r} (kN)	Theoretical failure load based on unstressed section, P_{ult}' (kN)			$\frac{P_{ult}}{P_{ult}'}$	$\frac{P_{ult-r}}{P_{ult}'}$	$\frac{P_{cr}}{P_{cr}'}$	$\frac{P_{cr}}{P_{ult}}$	$\frac{P_{cr}}{P_{ult-r}}$	$\frac{P_{cr}}{P_{ult}'}$	$\frac{P_{cr-r}'}{P_{ult}}$	$\frac{P_{ult-r}}{P_{ult}}$
					Steel yielding	Concrete crushing	Shear failure								
P1A,F	10.67	34.00	110.00	84.00	58.91	44.82	31.37	3.51	2.68	3.19	0.31	0.40	0.10	0.13	0.76
P2A,F	10.67	32.00	106.00	88.00	58.91	44.82	31.37	3.38	2.81	3.00	0.30	0.36	0.10	0.12	0.83
P3B,F	14.67	40.00	116.00	88.00	58.91	55.64	33.72	3.44	2.61	2.73	0.34	0.45	0.13	0.17	0.76
P4B,F	14.67	38.00	112.00	84.00	58.91	55.64	33.72	3.32	2.49	2.59	0.34	0.45	0.13	0.17	0.75
P5A,S	10.67	28.00	82.00	60.00	31.80	44.82	11.05	7.42	5.43	2.63	0.34	0.47	0.13	0.18	0.73
P6A,S	10.67	26.00	86.00	60.00	31.80	44.82	11.05	7.79	5.43	2.44	0.30	0.43	0.12	0.18	0.70
P7B,S	14.67	32.00	102.00	68.00	31.80	55.64	11.87	8.59	5.73	2.18	0.31	0.47	0.14	0.22	0.67
P8B,S	14.67	30.00	100.00	44.00	31.80	55.64	11.87	8.42	3.71	2.05	0.30	0.68	0.15	0.33	0.44
Average	**12.67**	**32.50**	**101.75**	**72.00**	**45.36**	**50.23**	**22.00**	**5.73**	**3.86**	**2.60**	**0.32**	**0.47**	**0.12**	**0.19**	**0.70**
P9A,F	10.67	34.00	106.00	70.00	58.91	44.82	31.37	3.38	2.23	3.19	0.32	0.49	0.10	0.15	0.66
P10B,F	14.67	40.00	116.00	72.00	58.91	55.64	33.72	3.44	2.14	2.73	0.34	0.56	0.13	0.20	0.62
P11A,S	10.67	26.00	82.00	44.00	31.80	44.82	11.05	7.42	3.98	2.44	0.32	0.59	0.13	0.24	0.54
P12B,S	14.67	32.00	102.00	50.00	31.80	55.64	11.87	8.59	4.21	2.18	0.31	0.64	0.14	0.29	0.49
Average	**12.67**	**33.00**	**101.50**	**59.00**	**45.36**	**50.23**	**22.00**	**5.71**	**3.14**	**2.63**	**0.32**	**0.57**	**0.13**	**0.22**	**0.58**
C1A,F	10.67	18.00	72.00		58.91	44.82	31.37	2.30		1.69	0.25		0.15		
C2B,F	14.67	20.00	68.00		58.91	55.64	33.72	2.02		1.36	0.29		0.22		
C3A,S	10.67	14.00	40.00		31.80	44.82	11.05	3.62		1.31	0.35		0.27		
C4B,S	14.67	16.00	56.00		31.80	55.64	11.87	4.72		1.09	0.29		0.26		
Average	**12.67**	**17.00**	**59.00**		**45.36**	**50.23**	**22.00**	**3.16**		**1.36**	**0.29**		**0.22**		

Table 3. Details of applied pre-stress forces to beams before load test

Beam No.	upward deflection due to prestress (mm)	Prestress causing Upward deflection, Pt (kN)	downward deflection due to selfweight (mm)	Prestress loss due to elastic shortening, Po (kN)	Loss of prestress due to Creep, Pc (kN)	Prestress At transfer, Pt (kN)
P1A,F	2.03	366.61	0.02	35.80	3.24	395.71
P2A,F	2.05	370.22	0.02	36.15	3.24	403.47
P3B,F	1.94	376.38	0.02	34.22	2.89	404.45
P4B,F	1.96	380.26	0.02	34.57	2.89	412.75
P5A,S	2.22	400.93	0.02	39.12	3.24	472.48
P6A,S	2.28	411.76	0.02	40.17	3.24	498.14
P7B,S	2.13	413.24	0.02	37.54	2.89	486.72
P8B,S	2.11	409.36	0.02	37.19	2.89	477.70
average	2.09	391.09	0.02	36.84	3.07	443.93
P9A,F	2.03	366.61	0.02	35.80	3.24	395.71
P10B,F	1.94	376.38	0.02	34.22	2.89	404.45
P11A,S	2.22	400.93	0.02	39.12	3.24	472.48
P12B,S	2.13	413.24	0.02	37.54	2.89	486.72
average	2.08	389.29	0.02	36.67	3.07	439.84

Table 4. Details of applied pre-stress forces to beams after collapse

Beam No.	upward deflection due to re-stress (mm)	Re-stress causing Upward deflection, Pt (kN)	downward deflection due to selfweight (mm)	Prestress loss, Po (kN)	Loss of prestress due to Creep, Pc (kN)	Restress At transfer, Pt (kN)
P1A,F	2.01	366.52	0.02	35.45	3.24	388.03
P2A,F	2.02	368.33	0.02	35.63	3.24	391.86
P3B,F	2.00	391.65	0.02	35.27	2.89	429.60
P4B,F	2.01	393.59	0.02	35.44	2.89	433.87
P5A,S	2.03	370.14	0.02	35.80	3.24	395.71
P6A,S	2.10	382.78	0.02	37.03	3.24	423.20
P7B,S	2.05	401.35	0.02	36.14	2.89	451.15
P8B,S	2.06	403.29	0.02	36.31	2.89	455.52
average	2.04	384.70	0.02	35.88	3.07	421.12
P9A,F	2.30	418.90	0.02	40.52	3.24	506.84
P10B,F	2.08	407.17	0.02	36.66	2.89	464.33
P11A,S	2.06	375.55	0.02	36.33	3.24	407.38
P12B,S	2.03	397.47	0.02	35.79	2.89	442.47
average	2.12	399.77	0.02	37.32	3.07	455.25

J. Load-deflection curves

Monotonic loading

Figures 3 and 4 show the load-deflection curves for the beams under monotonic loading. Failure loads for the beams before and after retrofit averaged over 100kN and 72kN respectively. Because the stressed F-series beams were stiffer and more ductile, they recorded higher failure loads. After retrofit, the average failure loads were 86kN and 58kN for F and S series respectively. The unstressed beams recorded the least failure loads averaging about 45kN. The retrofitted beams carried more load, showed a respectable degree of ductility though not as much as before retrofit. Due to the initial compressive stresses induced in the beams, they behaved more elastically than the unstressed beams. The maximum deflection at failure was 15mm and 12mm for F-series and S-series respectively.
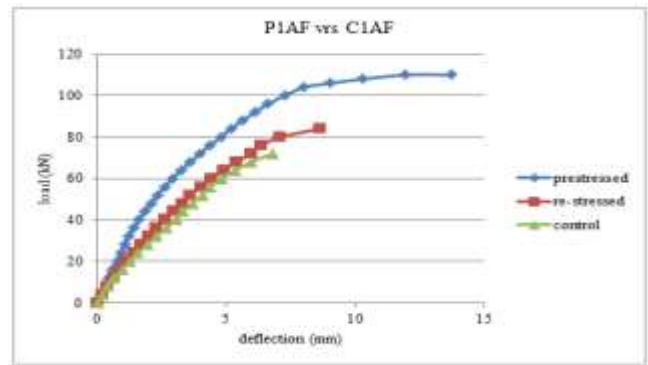

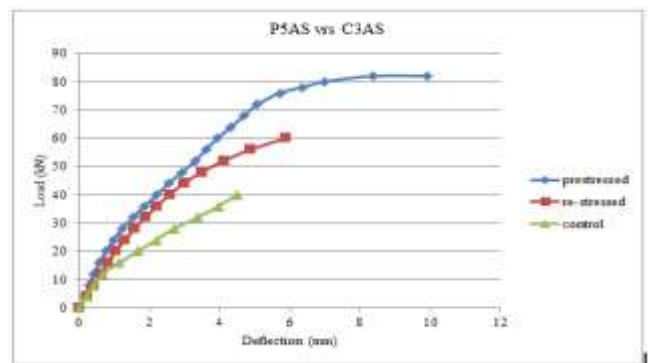Fig. 3. F-series beam under monotonic loading

Fig. 4. S-series beam under monotonic loading

Cyclic loading

Twenty load cycles were applied to beams P9 – P12 after retrofit, using their first crack loads as the cycle load. Figures 5 and 6 shows the load-deflection curves for beams P9 and P11 under cyclic loading in comparism with curves for their monotonic loading before retrofit and the monotonic loading of a control beam. The average first crack load was 33kN and the failure load after the 20 cycles of loading averaged 59kN. The ratio of the failure loads under cyclic loading averaged 100% and 58% relative to the control beams and the failure loads before retrofit respectively. It was observed during cycle loading that cracks closed completely upon load removal and re-opened upon load application. Before and after retrofit, the maximum crack width ranged between 0.03 and 0.2mm and 0.08 and 0.7mm respectively. That for the unstressed beams ranged between 2.00 and 4.00mm.
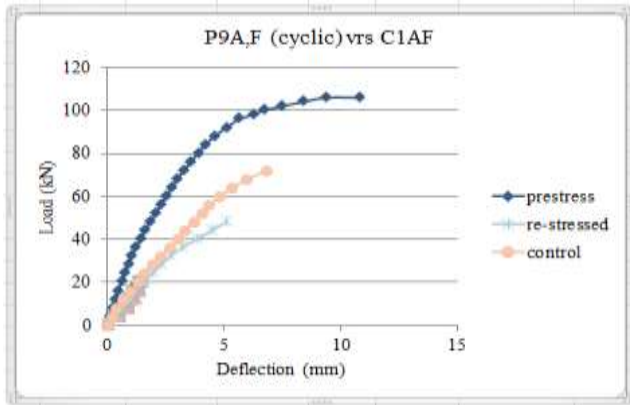
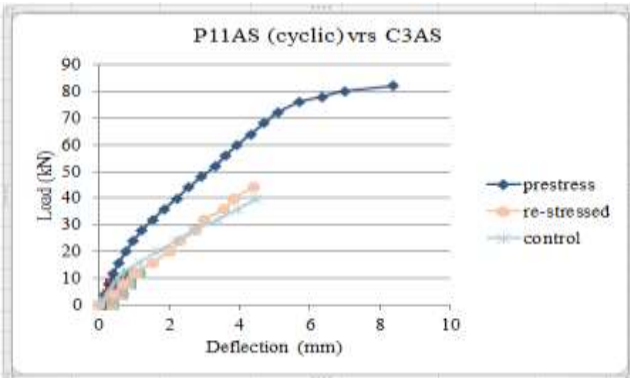Fig. 5. F-series beam under cyclic loading

Fig. 6. S-series beam under cyclic loading

Fig. 8. S-series beams failed in pure shear and flexure

Table 5. Details of cracks before and after retrofit

Beam No	Mode of Failure	Number and Type of cracks after retrofit	Max. crack width before retrofit (mm)	Max. crack width after retrofit (mm)
F1AF	Diagonal shear + Flexural compression	11 pure flexural + 3 shear + 1 diagonal shear	0.05	0.10
F2AF	Diagonal shear + Flexural compression	12 pure flexural + 4 shear	0.05	0.09
F3BF	Diagonal shear + Flexural compression	8 pure flexural + 2 shear + 1 diagonal shear	0.04	0.09
F4BF	Diagonal shear + Flexural compression	17 pure flexural + 3 shear + 1 diagonal shear	0.05	0.08
F5AS	Diagonal shear + Steel yielding	7 pure flexural + 2 shear	0.15	0.3
F6AS	Diagonal shear + Steel yielding	6 pure flexural + 3 shear	0.20	0.7
F7BS	Diagonal shear + Steel yielding	8 pure flexural + 2 shear	0.06	0.12
F8BS	Diagonal shear + Steel yielding	10 pure flexural + 2 shear	0.08	0.30
F9AF	Diagonal shear + Flexural compression	9 pure flexural + 3 shear	0.07	0.30
F10BF	Diagonal shear + Steel yielding	10 pure flexural + 2 shear + 2 diagonal shear	0.09	0.4
F11AS	Diagonal shear + Flexural compression	9 pure flexural + 4 shear	0.20	0.7
F12BS	Diagonal shear + Steel yielding	9 pure flexural + 2 shear + 1 diagonal shear	0.18	0.8
C1AF	Diagonal shear + Flexural compression	9 pure flexural + 3 shear	3.00	
C2BF	Diagonal shear + Steel yielding	9 pure flexural + 4 shear	3.10	
C3AS	Diagonal shear + Flexural compression	8 pure flexural + 4 shear	3.50	
C4BS	Diagonal shear + Steel yielding	10 pure flexural + 2 shear	3.10	

K. Failure modes

Collapse of the F-series beams occurred predominantly through diagonal shear as seen in Fig. 7, though they were expected to fail in flexure due to the presence of shear stirrups. It was observed however that the enhanced flexural capacity provided by the additional hanger bars together with a shear-span to effective depth ratio that fell between 2.5 and 6 pre-empted the shear failure [11]. The maximum diagonal shear crack width averaged 2.07mm while the pure flexural crack widths averaged 0.07mm.

The S-series beams without shear reinforcement and designed to fail in shear, failed in pure shear and flexure, and recorded less cracks as shown in Fig. 8. This suggested they were less ductile than the F-series beams. Crack widths for the S-series beams averaged 0.7mm. Table 5 gives the details of cracks before and after beam retrofit.

Fig. 7. F-series beams failed in diagonal shear predominantly

V. CONCLUSION

L. Load carrying capacity

The ratio of the experimental failure load over the theoretical failure load (P_{ult} / P_{ult}'), averaged more than 570% before retrofit and about 380% after retrofit (P_{ult-r}/P_{ult}'). The ratio of the experimental failure load after retrofit was about 70% of the failure load before retrofit (P_{ult-r}/P_{ult}). There was a 22% increase in the load carrying capacity of the retrofitted beams relative to the unstressed beams. However, under cyclic loading, the retrofitted beams compared equally with the unstressed beams. For the stressed beams, the ratio of first crack load over theoretical cracking load (P_{cr} / P_{cr}') averaged about 260%, equivalent to an increase of more than 1.5 fold.

M. Deflection Behaviour

The stressed beams in general and the F-series beams in particular were more ductile, took more loads and therefore deflected more both before and after retrofit. The initial compressive stresses induced in the beams caused them to be ductile while the unstressed control beams exhibited brittle behaviour by fracturing almost immediately the maximum load was reached.

N. Crack Development

Throughout the cyclic loading of the retrofitted beams, cracks closed up completely on removal of the applied load and re-opened whenever the load was re-applied invariably to the same level. This was due to the induced compressive stresses along the entire span of the beam and caused the retrofitted beams to behave in similar fashion as the control beams under cyclic loading but better under monotonic loading. Crack

widths were significantly smaller than those in the unstressed beams.

REFERENCES

[1] N. Anwar and F. A. Najam, "Chapter Seven - Retrofitting of Cross-Sections," in *Structural Cross Sections*, Butterworth-Heinemann, 2017, pp. 483–530.

[2] M. Aslam, P. Shafigh, M. Z. Jumaat, and S. N. R. Shah, "Strengthening of RC beams using prestressed fiber reinforced polymers – A review," *Constr. Build. Mater.*, vol. 82, pp. 235–256, May 2015.

[3] P. Balaguru, A. Nanni, and J. Giancaspro, *FRP Composites for Reinforced and Prestressed Concrete Structures*. 270 Madison Ave, New York, NY 10016, USA: Taylor & Francis, 2009.

[4] M. F. Belal, H. M. Mohamed, and S. A. Morad, "Behavior of reinforced concrete columns strengthened by steel jacket," *HBRC*, vol. 11, no. 2, pp. 201–12, 2015.

[5] H. N. Garden and L. C. Hollaway, "An experimental study of the failure modes of reinforced concrete beams strengthened with prestressed carbon composite plates," *Elsevier Sci. Ltd.*, vol. 8368, no. 97, pp. 411–424, 1998.

[6] H. Nordin and B. Täljsten, "Concrete beams strengthened with prestressed near surface mounted CFRP," *J Compos Constr*, vol. 10, no. 1, pp. 60–8, 2006.

[7] H. Peng, J. Zhang, C. S. Cai, and Y. Liu, "An experimental study on reinforced concrete beams strengthened with prestressed near surface mounted CFRP strips," *Eng. Struct.*, vol. 79, pp. 222–233, Nov. 2014.

[8] A. Shokoohfar and A. Rahai, "Prediction model of long-term prestress loss interaction for prestressed concrete containment vessels," *Arch. Civ. Mech. Eng.*, vol. 17, no. 1, pp. 132–144, Jan. 2017.

[9] C. K. Kankam, "Structural behaviour of bolted end-plated reinforced concrete beams," *Mater. Des.*, vol. 24, no. 5, pp. 367–375, Aug. 2003.

[10] BS 8110-1, "Structural use of concrete," 1985.

[11] ACI-ASCE Committee 426, "Shear strength of concrete members," in *Proc. ASCE, No. ST 6*, 1973, pp. 1091–1187.

Appendix A: Derivation of prestress force from central deflection

The resultant deflection at transfer caused by a combination of the prestress force (upward deflection) and the selfweight of the beam (downward deflection) as derived by [9] is given by:

Prestress force causing upward deflection:
$$y_1 = 5P_t e_o L^2 / (48E_c I) \tag{0.1}$$

The % prestress loss due to creep:
$$\% \text{ loss} = P_c / P_o \tag{0.2}$$

Hence at transfer
$$P_t = \{P_o / (P_c / P_0)\} = P_0^2 / P_c \tag{0.3}$$

Therefore
$$y_1 = 5 P_o^2 e_0 L^2 / (48 P_c E_c I) \tag{0.4}$$

Downward deflection due to selfweight:
$$y_2 = 5wL^4 / (384E_c I) \tag{0.5}$$

Resultant deflection is therefore given by
$$y = y_1 + y_2 = [5 P_o^2 e_o L^2 / (48 P_c E_c I)] - [5wL^4 / (384E_c I)] \tag{0.6}$$

where the minus sign is as a result of the two opposing deflections

P_c loss of prestress due to creep
P_o applied prestress force
P_t prestress at transfer

e_o eccentricity of applied prestress force from the centroidal axis of the beam
w unit weight of beam
E_c elastic modulus of concrete
I 2nd moment of area of the concrete section
L span

The creep prestress P_c is given by:
$$P_c = E_s (P_1 A_{st} / A) (1+e_o^2 A / I) \Phi \tag{0.7}$$
where
$$P_1 = P_o / \{(1 + \alpha_e A_{st} / A) (1+e_o^2 A / I)\} \tag{0.8}$$
$$\alpha_e = E_s / E_c \tag{0.9}$$
where

P_1 residual prestress force post loss due to concrete elastic contraction
E_s steel modulus of elasticity
Φ specific creep strain of concrete
α modular ratio
A concrete cross-sectional area
A_{st} steel cross-sectional area

From equations 4.6 to 4.8, the applied prestress force (P_o) comes to:
$$P_o = \{(9.6 \Phi E_c E_s I A_{st} / A) (y + 5wL^4 / 384 E_c I)\} / e_o L^2 \tag{0.10}$$
$$P_o = \{(9.6 \Psi E_s I A_{st} / A) (y + 5wL^4 / 384 E_c I)\} / e_o L^2 \tag{0.11}$$
where

Φ Ψ / Ec
Ψ creep coefficient = 1.4 (after 28 days)
E_c $9.1f_{cu}^{0.33}$
f_{cu} 28-day compressive strength of concrete